Hypoosmotic Expression of *Dunaliella bardawil* ζ-Carotene Desaturase Is Attributed to a Hypoosmolarity-Responsive Element Different from Other Key Carotenogenic Genes[1][C][W]

Yong-Min Lao, Lan Xiao, Li-Xin Luo, and Jian-Guo Jiang*

College of Food Science and Engineering, South China University of Technology, Guangzhou 510640, China (Y.-M.L., J.-G.J.); and School of Biological Science and Engineering, South China University of Technology, Guangzhou 510006, China (Y.-M.L., L.X., L.-X.L.)

Some key carotenogenic genes (*crts*) in *Dunaliella bardawil* are regulated in response to salt stress partly due to salt-inducible cis-acting elements in their promoters. Thus, we isolated and compared the ζ-carotene desaturase (*Dbzds*) promoter with other *crts* promoters including phytoene synthase (*Dbpsy*), phytoene desaturase (*Dbpds*), and lycopene β-cyclase1 (*DblycB1*) to identify salt-inducible element(s) in the *Dbzds* promoter. In silico analysis of the *Dbzds* promoter found several potential cis-acting elements, such as abscisic acid response element-like sequence, myelocytomatosis oncogene1 recognition motif, AGC box, anaerobic motif2, and activation sequence factor1 binding site. Remarkably, instead of salt-inducible elements, we found a unique regulatory sequence architecture in the *Dbzds* promoter: a hypoosmolarity-responsive element (HRE) candidate followed by a potential hypoosmolarity-inducible factor GBF5 binding site. Deletion experiments demonstrated that only HRE, but not the GBF5 binding site, is responsible for hypoosmotic expression of the *fusion of Zeocin resistance gene* (*ble*) to the *enhanced green fluorescent protein* (*egfp*) chimeric gene under salt stress. *Dbzds* transcripts were in accordance with those of *ble-egfp* driven by the wild-type *Dbzds* promoter. Consequently, *Dbzds* is hypoosmotically regulated by its promoter, and HRE is responsible for this hypoosmotic response. Finally, the hypoosmolarity mechanism of *Dbzds* was studied by comparing transcript profiles and regulatory elements of *Dbzds* with those of *Dbpsy*, *Dbpds*, *DblycB1*, and *DblycB2*, revealing that different induction characteristics of *crts* may correlate with regulatory sequence architecture.

Carotenoids are a structurally diverse class of isoprenoids synthesized by all photosynthetic organisms and many nonphotosynthetic organisms, such as certain species of bacteria, fungi, and archaea (Goodwin, 1980). They possess many advantageous properties for the human body on account of their vitamin A activity as essential nutrients (Farré et al., 2010), prevention and treatment functions against several kinds of diseases as health care products (Michaud et al., 2000; Landrum and Bone, 2001; Shaish et al., 2006), as well as industrial agents as colorants, forages, and cosmetics (Schmidt-Dannert, 2000). Therefore, the investigation of biosynthetic mechanisms and commercial exploitation of carotenoids have gained increasing attraction in many laboratories and companies. Recently, at least 700 carotenoids have been characterized from natural carotenoid biosynthetic pathways (Feltl et al., 2005).

Some carotenogenic microorganisms have been commercially employed to produce important carotenoids (Johnson et al., 1995; Raja et al., 2007). Among these microorganisms, the *Dunaliella* genus, especially *Dunaliella salina* and *Dunaliella bardawil*, has been researched extensively and exploited as a natural source of carotenoids due to its striking ability to accumulate carotenoids under certain circumstances (Amotz et al., 1982), including high light intensity, high salt concentration, and nutrient starvation. The carotenogenic pathway of *Dunaliella* species is a set of successional reactions from geranyl geranyl pyrophosphate (GGPP) to β-carotene, as shown in Figure 1 (Ye and Jiang, 2010). The first rate-limiting step is a head-to-head condensation of two GGPP molecules to produce phytoene by phytoene synthase (PSY; Salguero et al., 2005). Then, colorless phytoene undergoes four sequential desaturation reactions to synthesize the pink colorant pigment lycopene by carotene desaturase via the intermediates phytofluene, ζ-carotene, and neurosporene. In algae, higher plants, and cyanobacteria, carotenoid desaturation is sequentially fulfilled by phytoene desaturase (PDS) and ζ-carotene desaturase (ZDS; Matthews et al., 2003; Zhu et al., 2007). However, in bacteria and fungi, carotenoid desaturation is completed solely by *carotene*

[1] This work was supported by the National Natural Foundation of China (grant no. 31171631).

* Address correspondence to jgjiang@scut.edu.cn.

The author responsible for distribution of materials integral to the findings presented in this article in accordance with the policy described in the Instructions for Authors (www.plantphysiol.org) is: Jian-Guo Jiang (jgjiang@scut.edu.cn).

[C] Some figures in this article are displayed in color online but in black and white in the print edition.

[W] The online version of this article contains Web-only data.

www.plantphysiol.org/cgi/doi/10.1104/pp.114.235390

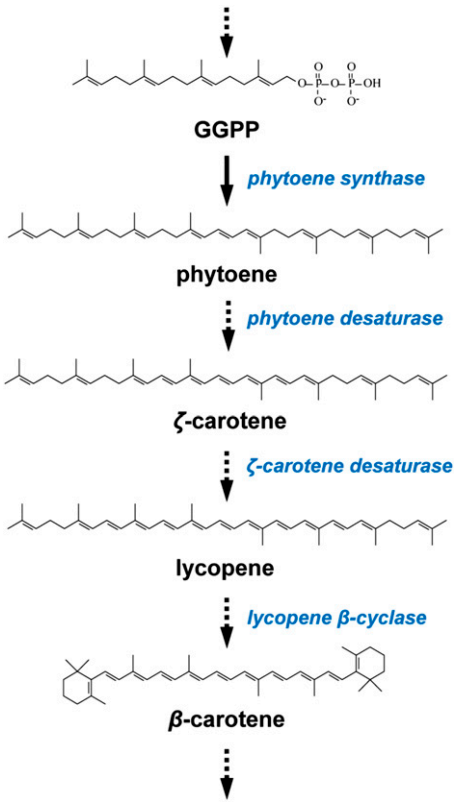

Figure 1. Abbreviated biosynthetic pathway of carotenoids from GGPP to β-carotene in *Dunaliella* spp. (Ye and Jiang, 2010). Commonly, the carotenogenic pathway is made up of three main parts: GGPP biosynthesis, lycopene generation, and the formation of carotenoids with cyclohexene and their derivatives. Metabolites are shown in boldface, whereas enzymes for relative conversions are displayed in italics. Dashed arrows represent one or more intermediates being generated under the catalysis of related enzymes. [See online article for color version of this figure.]

desaturaseI (*crtI*), which seems to have the property of catalyzing the cis-to-trans conversion of carotenes (Sandmann, 2009). Subsequently, β-carotene is formed through the β-cyclization of lycopene by lycopene β-cyclase (LYCB; Zhu et al., 2008).

Considering the important role of ZDS in the poly-cis-desaturation pathway, studies on its functions have been carried out (Linden et al., 1993, 1994; Bartley et al., 1999; Matthews et al., 2003; Bautista et al., 2005). ZDS was first cloned from *Anabaena* species (Linden et al., 1993) and then from pepper (*Capsicum annuum*; Albrecht et al., 1995) and prokaryotic cyanobacteria *Synechocystis* species (Breitenbach et al., 1998), which showed high similarity to the PDS-type desaturases. Heterologous expression experiments revealed an indispensable function of ZDS in the formation of lycopene (Bartley et al., 1999); mutation of the *zds* gene from Arabidopsis (*Arabidopsis thaliana*) could lead to increased superoxide generated from photooxidation, resulting in impaired carotenogenesis and subsequent spontaneous cell death (Dong et al., 2007b); it is also reported that the ZDS enzyme was involved in chloroplast development, photoprotection, and retrograde signaling (Bautista et al., 2005; Dong et al., 2007b). In sunflower (*Helianthus annuus*), *zds* expression is regulated during development, since a concurrent increase of *zds* transcript levels with light-dependent carotenoid biosynthesis in cotyledons was observed (Fambrini et al., 2004). The expression of *zds* from *Chlorella protothecoides* is up-regulated in response to light, implying a transcriptional regulatory basis involved in carotenogenesis (Li et al., 2011).

Despite the fact that ZDS is essential for carotenoid biosynthesis, cell growth, and development in plants, the regulation mechanisms in many algae are not so clear. At present, available information about ZDS in *D. salina* and *D. bardawil* is from our previous work, which is solely restricted to sequence characteristics (Ye and Jiang, 2010; Ye et al., 2011). Further knowledge on its regulation mechanisms for massive accumulation of β-carotene in response to salt stress remains to be discovered. Our previous study on the *D. bardawil psy* (*Dbpsy*) promoter region implied various regulatory elements involved in the transcriptional expression of the *Dbpsy* gene (Lao et al., 2011). It seems that the regulation of many key carotenogenic genes (*crts*) is partly attributed to related transcriptional regulatory elements residing in the promoter regions; therefore, in this study, we attempted to isolate the promoter and terminator of *Dbzds* and subsequently used them to express a fusion protein, fusion of Zeocin resistance gene (BLE) to the enhanced green fluorescent protein (EGFP), in *D. bardawil*. A database-assisted approach was used to identify potential cis-acting element candidates in the *Dbzds* promoter. A hypoosmolarity-responsive element (HRE) followed by a GBF5 binding site (GBF5BS) was found in the *Dbzds* promoter; such an architecture is common in many Arabidopsis L-Pro-inducible genes (Satoh et al., 2002, 2004). Thus, we detected the endogenous *Dbzds* transcripts in wild-type cells and exogenous *ble-egfp* driven by the wild-type *Dbzds* promoter (pZBET), HRE-deleted promoter (pDBET1), GBF5BS-deleted promoter (pDBET2), or HRE-GBF5BS-deleted promoter (pDBET3) in transgenic cell lines by real-time PCR under salt stress. Nearly opposite trends of transcriptional changes observed under salt stress between *Dbzds* or pZBET and pDBET1 or pDBET3 in wild-type cells or transgenic cell lines confirmed the role of HRE in the hypoosmotic response. We also detected and compared the transcript patterns and regulatory elements of *Dbzds* with those of *Dbpsy*, *Dbpds*, *DblycB1*, and *DblycB2*, with the purpose of determining the hypoosmolarity mechanism of *Dbzds* in response to salt stress.

RESULTS

The Effect of Salt Shock and Stress on Cell Growth and Nitrate Uptake

Coesel et al. (2008) reported that nutrient limitation, other than high light or salt stress, is the main regulatory

factor to affect *D. salina crts* expression by interfering with the interaction between cell growth and nitrate uptake. To address the role of nitrate and NaCl concentrations in *crts* expression in our study, we traced daily cell growth and nitrate content in the culture medium under salt stress. *D. bardawil* cells acclimated to 2 M NaCl for 10 d (exponential phase) were transferred to fresh medium at 0 to 4.5 M NaCl and subsequently cultivated for another 25 d (see "Materials and Methods"). Daily cell growth (Fig. 2) and nitrate content in each sample of different NaCl concentrations (Fig. 3) were measured after shifting.

D. bardawil cells cultivated in 2 M NaCl concentration showed a higher growth rate in comparison with other cultures; cells cultivated in 1 M NaCl concentration showed no significant differences from those in 2 M NaCl concentration, suggesting that *D. bardawil* cells can cope efficiently with the NaCl decrease from 2 to 1 M. The optimum salinity range for *D. bardawil* cell growth was 1 to 2 M NaCl, in which cells grew rapidly after 7 d. Despite the slower growth rate observed at the beginning (3 d), cells cultivated in 0 and 3 M NaCl concentrations started to grow from day 4. However, when salt concentration increased to extreme hyperosmolarity (4.5 M), cells began to grow even after 10 d and the growth rate decreased significantly. Although the growth rates of 0 and 3 M NaCl samples were lower than those of cultures grown in the optimum growth salinity range, these cultures showed better growth than cultures in 4.5 M NaCl concentration. Within 10 d after shifting in our study, *D. bardawil* cells of 0, 3, and 4.5 M were impacted by short-term salt shifting (salt shock). Cell growth of the 4.5 M sample was significantly repressed in the first 10 d. Similar cell growth arrest by salt shock was observed by Coesel et al. (2008), indicating that salt shock exerts a great impact on cell growth. But much higher cell vitality was obtained in our study; the cell growth rate in all samples was almost 10- to 20-fold those reported by Coesel et al. (2008). Nevertheless, under long-term salt shifting (salt stress) condition, cells recovered and, thus, growth was observed to be accelerated. For all samples, cells grew to log or late log phase after salt stress (cultivation for approximately 21 d). Therefore, to analyze the effect of salt stress on *crts* expression, 21-d cultures after shifting were used in further experiments.

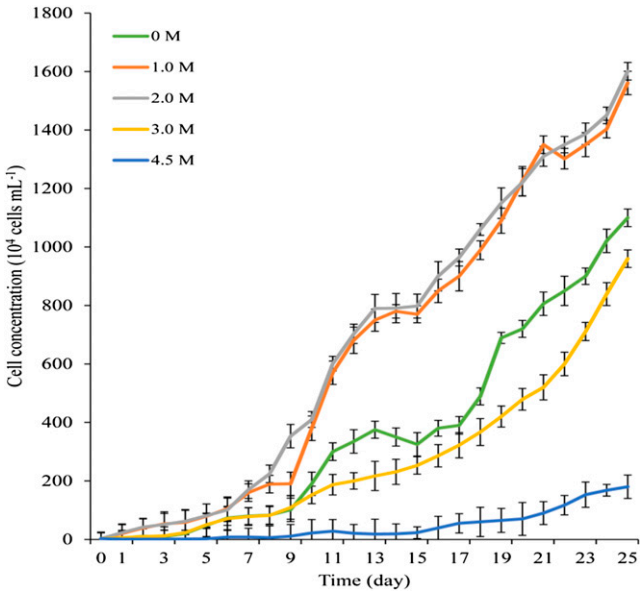

Figure 2. Cell growth curves of *D. bardawil* grown in a range of NaCl concentrations. The culture conditions and testing method were described in "Materials and Methods." Data points represent means of three replicated studies of each sample ± SD (Student's *t* test, $P < 0.05$). The correlation test showed that the growth of *D. bardawil* cells was significantly correlated with the salinity and incubation time ($P < 0.01$). One-way ANOVA showed that the growth of the three groups was significantly different at $P < 0.05$. [See online article for color version of this figure.]

The nitrate concentrations in the culture medium containing 0, 2, 3, and 4.5 M NaCl were consistent with the corresponding cell growth pattern (Fig. 3). A decrease of nitrate content could be observed in these samples as soon as 1 d after shifting. When cells grew exponentially (7–10 d; Fig. 2), consistently, the nitrate content in the medium dropped sharply in the 0, 2, and 3 M samples. The slower reduction rate of nitrate content in the 4.5 M sample in the first 6 d correlated with the slower growth rate of *D. bardawil* cells (Fig. 2). Then, nitrate content increased slightly in the 0, 2, and 3 M samples, while a clear, consistent reduction trend persisted in the 4.5 M sample. Salt shock exerted a significant impact on cell growth and nitrate uptake in the 4.5 M sample, such as cell growth arrest and, thus, slower nitrate uptake (Coesel et al., 2008). When cells had adjusted to the changes of salinity, cell growth recovered; therefore, nitrate uptake accelerated. However, because up to 5 mM KNO_3 (see "Materials and Methods") was used in the culture medium, which was sufficient for cells to flourish in all the conditions used here, nitrate depletion was not detected, as shown in Figure 3. Nitrate depletion significantly influences cell growth and *crts* expression (Coesel et al., 2008), and adequate nitrate minimizes such an effect. Actually, faster cell growth (Fig. 2) was obtained in our study due to sufficient nitrate supply, with cell numbers reaching approximately 10- to 20-fold those in nitrate-limiting or depletion conditions (Coesel et al., 2008).

Genomic Structure of *Dbzds*

The *Dbzds* gene of 6,879 bp contains 12 exons (E1, 1–139; E2, 399–541; E3, 742–821; E4, 1,058–1,142; E5, 1,477–1,660; E6, 2,013–2,225; E7, 2,694–2,889; E8, 3,144–3,293; E9, 3,653–3,755; E10, 3,963–4,169; E11, 4,623–4,824; E12, 6,389–6,879) interrupted by 11 introns (Supplemental Fig. S1). All introns are flanked by conventional 5′ splice donor GT and 3′ splice acceptor AG. Introns are often required for the full expression of genes in organisms such as yeast, plants, and animals.

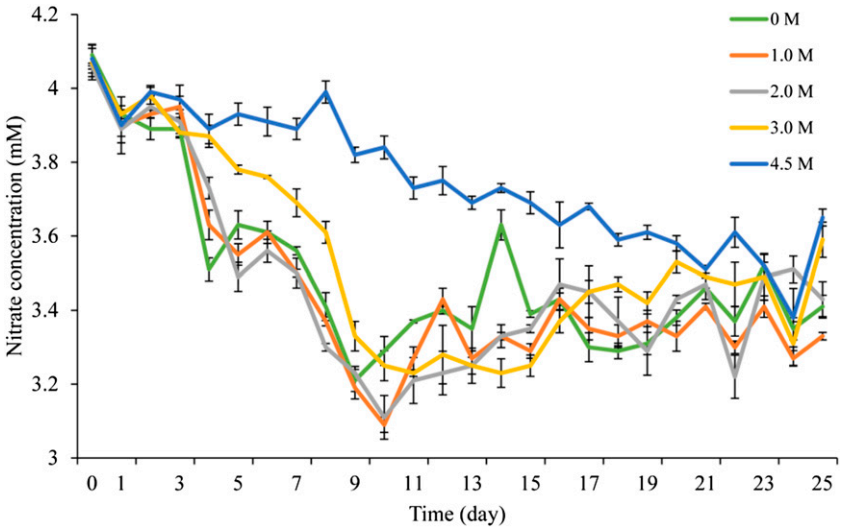

Figure 3. Effects of salt stress on dissolved nitrogen in *D. bardawil* culture medium. Nitrate concentrations in the medium were measured daily for 25 d after the salt shift. Data points represent means of three replicated studies of each sample ± SD (Student's *t* test, $P < 0.05$). The correlation test showed that the dissolved nitrogen in *D. bardawil* culture medium with different salinities was significantly correlated with the growth of *D. bardawil* and salinity ($P < 0.01$). (For the growth of *D. bardawil*, see Fig. 2.) One-way ANOVA showed that the nitrate contents of cultures at various salinities on each day were significantly different at $P < 0.05$. [See online article for color version of this figure.]

Introduction of the *ribulose-1,5-bisphosphate carboxylase small subunit2* (*rbcs2*) gene intron1 dramatically stimulated foreign gene expression in *Chlamydomonas reinhardtii* (Lumbreras et al., 1998). Sometimes intron location is conserved among species to endow crucial function preservation through evolution (Norris et al., 1993). We found one intron (I4, 1,143–1,476) that shares a similar location with the fourth intron (1,119–1,489) of *C. reinhardtii zds* (GenBank accession no. NW_001843867.1) The terminator of 959 bp was not predicted to contain any canonical poly(A) signal and transcriptional attenuator by the Signal Miner and RibEx programs (Abreu-Goodger and Merino, 2005). The promoter of this gene is 2,899 bp in length with typical GATA box (−126), CCAAT box (−743), and −300 elements (−801; TGAAAAAG glutenin gene conserved regulatory sequence). Several transcriptional regulatory elements were predicted as well (Supplemental Fig. S1). Remarkably, an HRE (which is designated as PRE in the PlantPAN database; −785), with a core 9-bp sequence (ACTCATCCT) necessary for the efficient expression of *proline dehydrogenase* (*proDH*) in response to L-Pro and hypoosmolarity (Satoh et al., 2002), is found in this *Dbzds* promoter. Moreover, GBF5BS, at −484 with consensus sequence ATGAGT, is also found in the *Dbzds* promoter. The expression of GBF5 is also induced by hypoosmolarity; thus, GBF5BS may also be necessary for L-Pro-responsive and hypoosmolarity-responsive expression of *proDH* in Arabidopsis (Satoh et al., 2002, 2004). A CpNpG island of 715 bp was calculated to immediately flank the transcriptional start site (A).

The *Dbzds* Promoter Contains Several Potential cis-Acting Elements

We used the PlantPAN server to exploit potential cis-acting elements in the *Dbzds* promoter to further investigate its regulation mechanisms for the inducible biosynthesis of β-carotene. According to the server's instructions, we selected six species: Arabidopsis, maize (*Zea mays*), rice (*Oryza sativa*), soybean (*Glycine max*), tomato (*Solanum lycopersicum*), and wheat (*Triticum aestivum*). We found several putative cis-acting elements/motifs that potentially conferred inducible features to the *Dbzds* promoter. These features are closely relevant to the documented regulatory properties of carotenogenesis in *D. bardawil*, such as light-, cold-, and pathogenesis-related regulation. Although the authenticity of these calculated cis-acting elements should be verified through further mutation experiments, data mining of possible regulatory motifs utilizing bioinformatics tools would supply valuable information for such experiments (Girin et al., 2007; Wang et al., 2010).

A putative abscisic acid response element (ABRE)-like sequence with consensus sequence ACGTG is found in the *Dbzds* promoter from −310 to −306, which was previously demonstrated to be essential for the induction of non-abscisic acid (ABA)-mediated responses to dehydration stress, in cooperation with a myelocytomatosis oncogene1 (MYC-1) recognition motif in Arabidopsis (Simpson et al., 2003). Actually, two MYC-1 recognition motifs (one from −2,698 to −2,693, the other from −2,302 to −2,297, with consensus sequence CAATTG) are also found in this *Dbzds* promoter. MYC-1 recognition motif was first found in the promoters of genes that are responsive to dehydration (*rd22*) and many other genes in Arabidopsis. It is the binding site of INDUCER OF CBF EXPRESSION1 in the CBF3 promoter, which regulates the transcription of *C-Repeat* (*CRT*)/*dehydration responsive element* (*DRE*) *binding proteins1* (*CBF*/*DREB1*) genes in the cold in Arabidopsis (Chinnusamy et al., 2003). The AGC box (−386; AGCCGCC) was first found in a 61-bp enhancer element in a *Nicotiana plumbaginifolia* class I β-1,3-glucanase gene (Hart et al., 1993) and in many basic pathogenesis-related genes (Cheong et al., 2003). However, the up-regulation or down-regulation responses of the AGC box to stress signals is dependent on the protein factors binding in Arabidopsis (Fujimoto et al.,

2000). Anaerobic motif2 (−1,718; AGCAGC) is found in silico in promoters of 13 anaerobic genes involved in the fermentative pathway in plants (Mohanty et al., 2005) as well as in *C. reinhardtii* (Ding et al., 2012). The activation sequence factor1 (ASF1) binding site (−1,839; TGACG) is identical to the TGACG motif, which is the binding site of the ASF1 in the cauliflower mosaic virus 35S promoter (Lam et al., 1989). The TAGCG motif is found in the high-mobility group (HMG)-box protein1 (HBP1) binding site of the wheat histone H3 gene and in many promoters to transcriptionally activate their host gene in response to auxin and/or salicylic acid (Després et al., 2003). It may be relevant for light regulation. ASF1 binds to two TGACG motifs (Lam et al., 1989).

Remarkably, a Pro-responsive element or HRE with a consensus sequence of ACTCAT is found in the promoter region at −785. It was first found in the *proDH* promoter in Arabidopsis, with a core sequence of ACTCATCCT indispensable for the efficient expression of *proDH* in response to L-Pro and hypoosmolarity (Satoh et al., 2002). It is believed that the subgroup of basic region/leucine zipper Arabidopsis transcription factors binds to this motif to function as a transcriptional activator for hypoosmolarity-inducible *proDH* in Arabidopsis (Satoh et al., 2004). Simultaneously, a potential hypoosmolarity-inducible factor, GBF5BS (−484; ATGAGT), which is commonly coupled with upstream HRE in many L-Pro-inducible genes (Satoh et al., 2002, 2004), is also found downstream of HRE in this *Dbzds* promoter. GBF5 is another subgroup of bZIP transcription factors that is hypoosmolarity inducible in Arabidopsis (Satoh et al., 2004). Carotenoid biosynthesis is largely enhanced by salt stress, especially under high salinity. It is reasonable to believe that many key CRTs in the β-carotene biosynthesis pathway should be induced under high salinity to launch β-carotene accumulation. Accompanied by high salinity, hyperosmolarity is imposed upon *D. bardawil* cells and thus triggers β-carotene production. At present, we still do not know the role of hypoosmolarity for carotenogenesis in *D. bardawil*. To uncover the true functions of these two potential cis-acting elements, we carried out further research, concentrating on these two elements.

The Obtained Sequence Is an Authentic Promoter of *Dbzds* with Expression Activity

To confirm the expression activity of the *Dbzds* promoter, we used it to drive an exogenous EGFP protein in *D. bardawil* cells. We constructed an EGPF expression vector, pZET, driven by the *Dbzds* promoter and terminated by the *Dbzds* terminator, and the negative expression vector pET absent of any promoter region. Transformed cells were incubated in the dark for 12 h to recover cell viability after transformation with pZET or pET vector, and then cells were incubated in the normal culture condition. Fluorescence images were obtained at days 2 and 21 after electrotransformation. Only red fluorescence appeared in cells transformed with the negative control vector pET deficient in the *Dbzds* promoter (Supplemental Fig. S2B), as in wild-type cells transformed with water in place of any vector (Supplemental Fig. S2A); however, moderate green fluorescence was observed as soon as 2 d after electroporation manipulation with pZET vector (Supplemental Fig. S2C). These results indicated that the foreign EGFP protein is transiently expressed by the *Dbzds* promoter in *D. bardawil* cells.

Subsequently, pZBET plasmid containing the Zeocin resistance gene *ble* (Drocourt et al., 1990) fused upstream of the *egfp* initiation codon ATG was constructed (Fig. 4) and transformed into *D. bardawil* cells to acquire heritable nuclear transformants. Small green colonies grown on Zeocin selective plates were transferred to Zeocin selective liquid medium for long-term cultivation (Supplemental Fig. S3A). Passage cells were also spread onto Zeocin selective plates (Supplemental Fig. S3B). A single colony was transferred to Zeocin selective liquid medium for subsequent cultivation. Zeocin resistance cells of log or late log phase were detected by fluorescence imaging, PCR, and reverse transcription (RT)-PCR assay. An expected product of 530 bp was permanently detected by PCR and RT-PCR amplification from primary cells (day 21) and passage cells (day 42), while no band was detected from the negative control pET-transformed cells on day 21 (Supplemental Fig. S3, C and D). Finally, this product was confirmed to be the *ble-egfp* fragment by sequencing. The *ble-egfp* fragment is preserved and transcribed in the transformants. Stronger green fluorescence was observed on both days 2 and 21 after transformation when Zeocin was used as selective

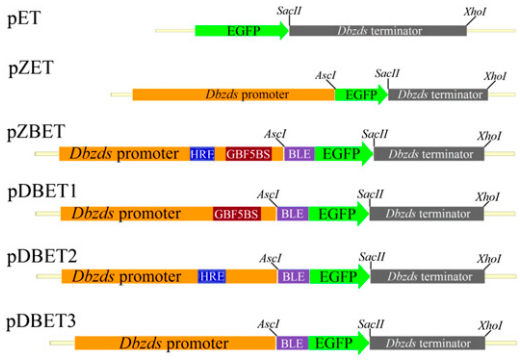

Figure 4. Constructs used to confirm the hypoosmolarity expression of *Dbzds* in this study. The transient expression vector pZET was constructed to validate the *Dbzds* promoter. Splice overlap extension-PCR was utilized to produce the *ble-egfp* chimeric gene, HRE-deleted promoter, GBF5BS-deleted promoter, and HRE-GBF5BS-deleted promoter, and subsequently, the resultant vectors pZBET, pDBET1, pDBET2, and pDBET3 were generated, respectively. The negative expression vector pET was also constructed. All fragment features are drawn to scale with the exception of HRE and GBF5BS elements. [See online article for color version of this figure.]

pressure (Supplemental Fig. S2, D and E). We also detected the expression of EGFP in passage cells; stable green fluorescence appeared sustainably in the second generation (Supplemental Fig. S2F). Therefore, heritable nuclear transformants are obtained and stable expression of the fusion protein BLE-EGFP by the *Dbzds* promoter is achieved. These observations strongly suggest that plasmid DNA is delivered into the nuclei of *D. bardawil* cells and transcribed and stable expression of *ble-egfp* is obtained. The authenticity of the *Dbzds* promoter is eventually confirmed to display strong activity.

ACTCATCCT Is Responsible for Hypoosmotic Expression of the *Dbzds* Promoter

In silico analysis of the *Dbzds* promoter found two interesting noticeable cis-acting elements potentially involved in hypoosmolarity expression of the *Dbzds* gene. One, designated as HRE, proved to be responsible for the hypoosmotic expression of its host gene *proDH* in Arabidopsis (Satoh et al., 2002). GBF5BS, with ATGAGT, is found downstream of HRE in *proDH*; although it has not been identified to participate in hypoosmolarity yet, the evidence implied its hypoosmotic feature, owing to (1) its coexistence in many L-Pro-inducible genes (Satoh et al., 2002) and (2) ATGAGT is the potential binding site of the hypoosmolarity-inducible GBF5 (Satoh et al., 2004). Hence, we deleted the HRE and/or GBF5BS and compared the *ble-egfp* transcripts prompted by these deleted and wild-type promoters under different NaCl concentrations. Here, the HRE-deleted vector is designated as pDBET1, pDBET2 refers to the GBF5BS deletion, and simultaneous deletion of HRE and GBF5BS is designated as pDBET3 (Fig. 4).

Initially, we traced the endogenous *Dbzds* transcriptional levels in wild-type cells cultivated in different NaCl concentrations ranging from 0 to 4.5 M. The obvious decline of *Dbzds* transcripts from hypoosmolarity (0 M) to hyperosmolarity (4.5 M) indicated the hypoosmotic expression of *Dbzds* in vivo (Fig. 5). Under hypoosmolarity conditions, *Dbzds* transcripts reached the maximum, whereas they fell to approximately 34.46% hypoosmolarity when NaCl concentration decreased to 2 M. Although a slight increase was observed in both 3 and 4.5 M NaCl samples compared with 2 M, it did not make the hypoosmotic expression of *Dbzds* ambiguous. In vivo, *Dbzds* is hypoosmolarity regulated at the transcriptional level.

When exogenous *ble-egfp* was expressed by the *Dbzds* promoter (pZBET) in *D. bardawil* cells, a similar profile to that of endogenous *Dbzds* transcripts was present. A distinct decrease of *ble-egfp* transcripts followed the elevated NaCl concentrations (Fig. 6). A lower transcript level of about 0.2384 times was observed in the 1 M salt sample against the hypoosmotic sample (0 M). When NaCl concentration increased to 2 M, a significant decrease of transcripts (34.91% hypoosmolarity) emerged. A similar trend was also displayed with the 3 and 4.5 M samples. The *ble-egfp* transcripts were enhanced by hypoosmolarity. The hypoosmotic expression of exogenous *ble-egfp* driven by the *Dbzds* promoter conformed to endogenous *Dbzds* in vivo, indicating that the HRE candidate in the *Dbzds* promoter discovered by PlantPAN might be responsible for the hypoosmotic expression of its host *Dbzds* gene.

In comparison with samples transformed with pZBET vector, the hypoosmotic expression trend of *ble-egfp* driven by the HRE-deleted promoter (pDBET1) was lost in the 0 M salt sample (Fig. 6). Significantly, 1.6121 times higher transcripts appeared in the 2 M sample than in the hypoosmotic sample (0 M). Despite a slight decline of transcripts in the 1 M sample, a different expression pattern from the wild-type promoter samples (pZBET) demonstrated that the hypoosmotic expression feature was lost after HRE was deleted; the

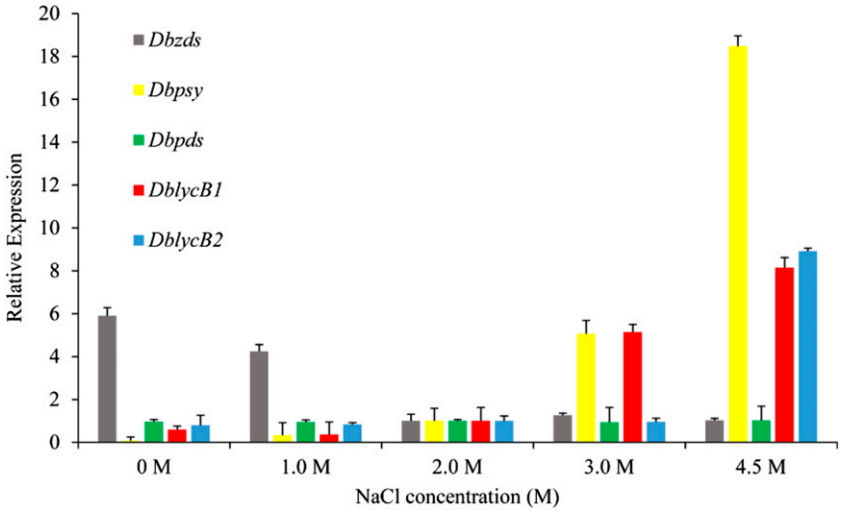

Figure 5. Several *crts* transcripts in response to NaCl stress. About 10^6 exponential phase (10-d) cells cultivated in the normal condition were transferred to corresponding medium with different NaCl concentrations and cultivated for another 21 d (log or late log phase). Immediately, approximately 10^7 cells were used for real-time quantitative PCR experiments (see "Materials and Methods"). Five key enzyme genes, *Dbpsy*, *Dbpds*, *Dbzds*, *DblycB1*, and *DblycB2*, were investigated. The known rate-limiting *Dbpsy* is significantly stimulated under hyperosmolarity, while *Dbzds* is hypoosmotically expressed in low- or no-NaCl medium. Expression values are given as ratios relative to the values of *D. bardawil glyceraldehyde-3-phosphate dehydrogenase*. All data are means of values obtained from three parallel experiments ± SD (Student's *t* test, $P < 0.01$). [See online article for color version of this figure.]

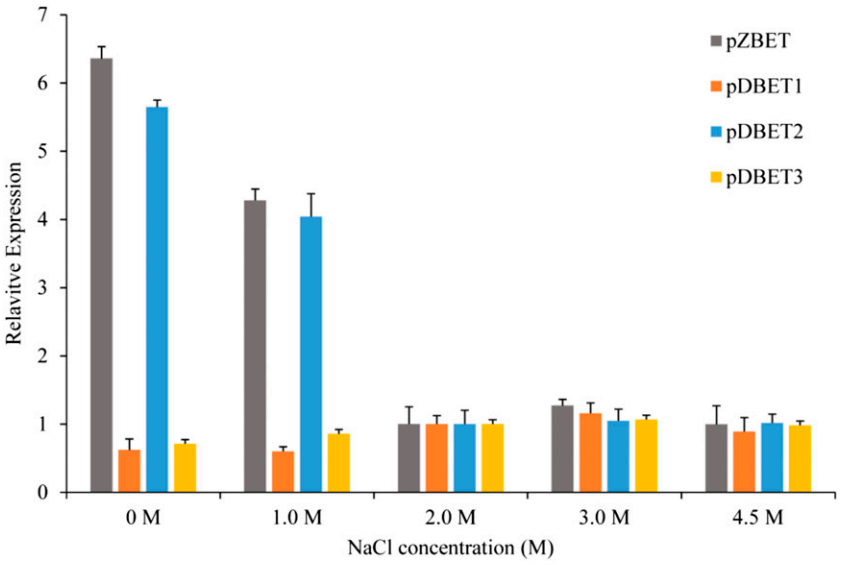

Figure 6. Expression patterns of *ble-egfp* driven by wild-type- or element-deleted *Dbzds* promoter. Consistent with in vivo *Dbzds* gene (Fig. 5), *ble-egfp* is down-regulated by wild-type (pZBET)- or GBF5BS-deleted *Dbzds* promoter (pDBET2): under the hypoosmotic condition (0 M NaCl), *ble-egfp* is significantly stimulated, and it shows clearly decreased trend of mRNA level when the NaCl concentration is elevated. Whereas, the mRNA level of *ble-egfp* driven by HRE (pDBET1)- or HRE-GBF5BS-deleted *Dbzds* promoter (pDBET3) loses this decreased trend when the NaCl concentration is elevated. Expression values are given as ratios relative to the values of *D. bardawil glyceraldehyde-3-phosphate dehydrogenase*. All data are means of values obtained from three parallel experiments ± SD (Student's *t* test, $P < 0.05$) [See online article for color version of this figure.]

HRE sequence ACTCATCCT is thus required for the hypoosmotic expression of *Dbzds* at the transcriptional level.

However, the GBF5BS-deleted samples did not affect exogenous *ble-egfp* transcripts. Using the GBF5BS-deleted promoter (pDBET2) to express *ble-egfp*, the transcriptional outline was in accordance with that of wild-type pZBET generally. Simultaneous deletion of both HRE and GBF5BS did not interfere with the trend that also appeared in pDBET1 (i.e. *ble-egfp* transcripts in pDBET3 were overall similar to those of pDBET1). Neither pDBET1 nor pDBET3 exerted a significant influence on *ble-egfp* transcripts in vivo. These results ruled out the synergistic effect of HRE and GBF5BS. GBF5BS is not an authentic cis-acting element for the hypoosmotic expression of *Dbzds*. Given all these observations, *Dbzds* is hypoosmotially expressed exclusively by HRE with core sequence ACTCATCCT, but not by GBF5BS.

DISCUSSION

CRTs Are Species-Specifically Regulated in Response to Salt Stress

Salinity stress could lead to an increase in the lycopene content of some tomato genotypes, implying enhanced expression of some CRTs upstream of LYCB (Borghesi et al., 2011). However, total carotenoid content prompted by salt stress does not always positively correlate with the induction of CRTs. A substantial decrease of total carotenoid content coupled with consistent increases of *psy*, *pds*, and *zds* in the callus of *Scutellaria baicalensis* was observed with increasing NaCl concentration (Tuan et al., 2013). In tomato, for reactions involving PSY, PDS, ZDS, and LYCB, there are no correlations between gene expression, enzyme activities, and metabolites (Fraser et al., 2007), while high light enhances zeaxanthin accumulation and induces *pds* expression simultaneously in *Chlorella zofingiensis* (Li et al., 2009). It appears that some CRTs are regulated independently of carotenoid accumulation in response to salt stress in a species-specific manner. Such a regulatory response may be rooted in transcriptional and/or posttranslational alterations (Walter and Strack, 2011).

In order to clarify these transcriptional alterations, we detected five pivotal *crts* transcripts under salt stress. Indeed, we found that *Dbpsy* and *DblycB1* are up-regulated by salt stress (Fig. 5). Under hypersalinity (3 M), the *Dbpsy* transcript showed significant augmentation, which reached its peak in extreme hypersalinity (4.5 M). The expression decline of *Dbpsy* with decreasing NaCl concentrations shrank to a minimum in extreme hyposalinity (0 M). These results indicated the rate-limiting role of *Dbpsy* in controlling carbon flux into the carotenogenesis pathway (Maass et al., 2009). It is reported that *D. bardawil* possesses two *psy* paralogs (Tran et al., 2009). Although no evidence at present shows differential regulation among *Dunaliella* species *psy* paralogs in response to salt stress, the possession of two *Dbpsy* paralogs might facilitate the fine-tuning of carotenogenesis at different stages of *D. bardawil* cell development or in response to different environmental stimuli, since differentially regulated *psy* paralogs in tomato (Fraser et al., 1999), *Citrus* species (Ikoma et al., 2001), maize (Li et al., 2008), and rice (Welsch et al., 2008) were found. Tomato and *Citrus* species possess two *psy* genes; chromoplast-specific *psy1* in both species is responsible for carotenoid biosynthesis in ripening fruit but barely contributes to the formation of carotenoids in chloroplast-containing tissues, while chloroplast-specific *psy2* mainly participates in foliar carotenoid formation (Fraser et al., 1999; Ikoma et al., 2001). Also, maize *psy3* (*Zmpsy3*) is up-regulated with the increase of carotenoid flux in response to salt stress in root and embryo tissue, whereas no changes were seen for *Zmpsy1* and *Zmpsy2* (Li et al.,

2008). Similarly, the expression of rice *psy3* (*Ospsy3*) is greatly activated by salt and drought, especially in root; despite moderate sensitivity to salt, *Ospsy2* as well as salt-insensitive *Ospsy1* are induced by light instead of salt stress (Welsch et al., 2008). Poaceae *psy3* and Solanaceae *psy1* seem to be the key regulators of carotenoid biosynthesis in response to salt stress in nonphotosynthetic tissue. At present, we cannot compare *Dbpsy* paralogs due to the unsuccessful cloning of another *Dbpsy* paralog in this strain, but the salt-inducible characteristic of a *Dbpsy* paralog (GenBank accession no. EU328287.1) analyzed here gives us a hint of the differential regulation between *Dbpsy* paralogs in response to different environmental stimuli and/or in different developmental stages.

Clear differences between *DblycB1* and *DblycB2* in most of the salinity spectrum ranging from 0 to 3 M, with the exception of extreme hypersalinity (4.5 M), under which both were substantially induced, indicated that the *DblycB* paralogs are differentially regulated and play different roles in carotenogenesis under different salinities. In comparison with *DblycB1*, repressed in lower salinities (0–1 M) than the control (2 M), *DblycB2* transcripts maintained a basal level similar to that of the control, suggesting a constitutive role in carotenoid biosynthesis under most salinity conditions. Like *psy*, tomato contains two *lycB* paralogs. The chloroplast-specific type *lycB1* is active in green tissue (Pecker et al., 1996), while the chromoplast-specific type *lycB2* is largely expressed in fruit (Ronen et al., 2000); this is proposed to be an ortholog of the pepper gene evolved from a common ancestor of *lycB1* after gene duplication (Hirschberg, 2001). Although there is a lack of evidence of plant *lycB* regulation in response to salt stress at present, for the above reasons, similar regulation to *psy* paralogs might be true for *DblycB*, especially in *DblycB1*, due to its transcriptional pattern that is more comparable to that of *Dbpsy* analyzed here (Fig. 5).

Currently, elucidation of ZDS regulation in response to salt stress is hindered by the lack of findings of salt impact on ZDS in *Dunaliella* species. In plants such as *S. baicalensis*, some tomato species, and sweet potato (*Ipomoea batatas*), ZDS is characterized to be salt inducible (Babu et al., 2011; Duan et al., 2012; Kim et al., 2013; Tuan et al., 2013). Conversely, *Dbzds* is down-regulated by salt stress in *D. bardawil* (Fig. 5). *Dbzds* is significantly induced by hyposalinity, while sustained steady expression levels approximate to that of the control in hypersalinity, suggesting its crucial role in basal carotenoid biosynthesis. The similar profile of *ble-egfp* transcripts driven by the *Dbzds* promoter further confirms this down-regulation under salt stress (Fig. 6). A decrease of *zds* transcripts is also observed in the leaves of tomato (cv PKM 1) under salt stress (Babu et al., 2011). ZDS seems to be differentially regulated by different mechanisms from PSY, PDS, and lycopene, to some extent. Evidence from *Narcissus pseudonarcissus* flowers also showed that 2-(4-chlorophenylthio)triethylamine hydrochloride induces PSY, PDS, and lycopene at the transcriptional and protein levels but exerts no effect on ZDS at both levels (Al-Babili et al., 1999). Unlike the effect of 2-(4-chlorophenylthio) triethylamine hydrochloride on these enzymes from *N. pseudonarcissus* flowers, the light-dependent enhanced carotenoid production in sunflower chloroplasts is accompanied by increased *zds* transcript levels (Fambrini et al., 2004), while *psy*, *pds*, and *zds* from pepper are independent of total carotenoid levels (Simkin et al., 2000). In contrast, low expression of *psy*, *pds*, and *zds* in leaves of tomato plantlets was detected with high carotenoid levels (Simkin et al., 2003).

Unlike the *crts* discussed above, *Dbpds* appears to be salt insensitive under all NaCl concentrations. When *Dbpds* transcripts in all samples were maintained at a level comparable to that of the control, no significant changes were observed (Fig. 5). PDS is also species-specifically regulated like other CRTs in plants and algae. In maize and foxtail millet (*Setaria italica*), salt stress does not affect PDS (Li et al., 2008; Veeranagamallaiah et al., 2008). Proteomic analysis of salt-stressed foxtail millet seedlings revealed that PDS is expressed in all NaCl concentrations (Veeranagamallaiah et al., 2008), while *S. baicalensis pds* transcripts were consistently increased with increasing NaCl concentrations (Tuan et al., 2013). Rather than high salt, *C. zofingiensis* PDS is induced by high light with light-dependent zeaxanthin accumulation, and although canthaxanthin and astaxanthin accumulate upon both stresses, high salt cannot impact PDS expression (Li et al., 2009). In *Haematococcus pluvialis*, PDS is also regulated by nitrate deprivation and light stress (Grünewald et al., 2000). However, both mRNA and protein levels of DbPDS remain constant in the high-light condition (Rabbani et al., 1998). *Dunaliella* species *pds* seems to be constitutive (Sun et al., 2008). It is believed that this striking difference between these two Volvocales species might be caused by the different localizations of the final product (Rabbani et al., 1998; Grünewald et al., 2000). In *D. bardawil*, carotenoids are synthesized exclusively within plastids and regulated by triacylglycerol droplets, but *Dbpds* is not induced at the transcriptional (Fig. 5) or translational level (Rabbani et al., 1998). *H. pluvialis* is unique in that carotenoid accumulation occurs in lipid vesicles outside the plastid with increasing PDS expression levels (Grünewald et al., 2000). As discussed below, we could not find any salt-inducible cis-acting element candidates in the *Dbpds* promoter compared with *Dbpsy*, *Dbzds*, and *DblycB1*. Therefore, the question now is whether the salt insensitivity of *Dbpds* is attributed to the sublocalization of carotenoid products and/or the absence of salt-inducible elements in this alga. Ongoing work to answer these questions is our current concern.

CRTs of *Dunaliella* Species Are Regulated Differentially at the Transcriptional Level

Previously, osmotic stress was thought to be independent of de novo protein synthesis, which induces existing enzymes to adjust to the new osmotic regime

(Sadka et al., 1989). However, Borowitzka et al. (1990) suggest that at least several CRTs of the carotenoid biosynthetic pathway need to be induced. Recent studies on the osmotic characteristics of *Dunaliella* species caused by salt stress classified the osmotic response into three stages, immediate response, short-term response, and long-term response, and found that long-term response mainly referred to osmotic stress-induced gene expression and salt-induced protein accumulation (Chen and Jiang, 2009). Under salt stress, long-term osmotic response is stimulated, and some salt-induced genes, including three *crts* analyzed here, are boosted under salt stress (Fig. 5). The first rate-limiting *psy* and paralog *lycB1* were significantly improved under hyperosmolarity in *D. bardawil* cells cultivated in nutrition-supplemented medium (Fig. 5). Enormous transcripts of *Dbpsy* and *DblycB1* activated by salt stress demonstrate that they might be at the crucial junction in the carotenogenesis pathway conserved in many species (Steinbrenner and Linden, 2001; Welsch et al., 2008; Tran et al., 2009).

Otherwise, *Dbpds* did not respond to salt stress (Fig. 5). *Dbpds* seems not to be the key regulatory point in β-carotene biosynthesis under salt stress in this alga. Nevertheless, *pds* transcripts are substantially stimulated in *D. salina* cells shifted to high light or high salt under nutrient-limiting conditions (Coesel et al., 2008). It is believed that nutrient limitation mainly contributes to the induction of *pds* in *D. salina*, since nitrate depletion appeared in the culture medium, which significantly impacted cell growth and gene expression (Coesel et al., 2008). The contradiction between Coesel et al. (2008) and our findings may result from the following reasons. (1) Unlike Coesel et al. (2008), who used 1.2 mM $NaNO_3$ as a nitrogen source, nutrition-supplemented (5 mM KNO_3) medium was used in our study to supply sufficient nitrate under all salt stress conditions; in fact, more than 3 mM nitrate was detected throughout our experiments in all salt stress samples (Fig. 3), so the impact of nitrate limitation or depletion on *crts* expression could be eliminated. (2) By measuring the cell growth rate in different salt stresses, almost uniform growth status (log or late log phase) was used for gene expression analysis in all samples; consequently, *crts* induction was mainly caused by salt stress in our study. (3) Another possibility for the contradiction between these two species could be that the induction of *pds* transcripts appears to be species specific within the genus *Dunaliella*.

In comparison with *Dbpsy* and *DblycB1*, *Dbzds* transcripts are tremendously promoted by hyposalinity (Fig. 5). At present, no further information on the hypoosmotic expression of *zds* transcripts is reported in the genus *Dunaliella*. However, transcription inhibitors prevent the substantial accumulation of β-carotene upon high light in *D. salina* cells grown at high salinity (Lers et al., 1990). These observations strongly suggest that some *crts* may be regulated differentially in response to salt stress at the transcriptional level, and *zds* transcripts might be differentially induced by salt when compared with other key *crts* of *Dunaliella* species.

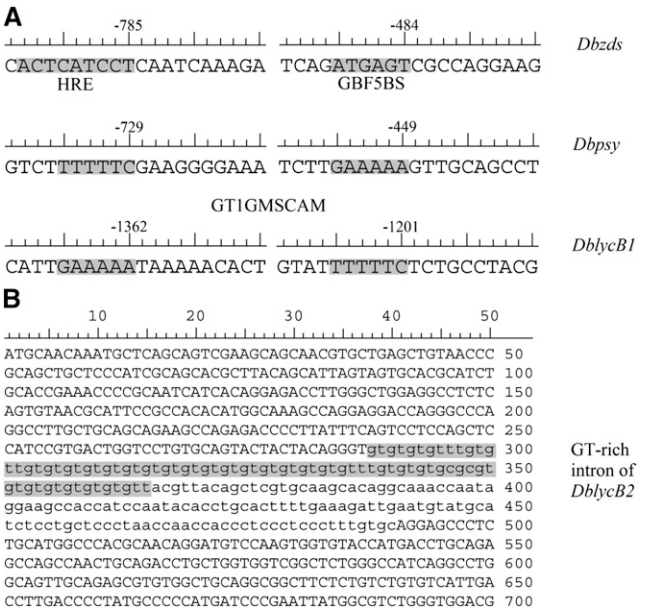

Figure 7. Differential regulatory sequence architectures of four *crts* in *D. bardawil*. A, GT-1 motifs are exclusively found in both *Dbpsy* and *DblycB1* promoters and are potentially responsible for hyperosmotic expression of these two *crts*, while HRE is only found in the *Dbzds* promoter to give hypoosmotic expression of *Dbzds*. The predicted complementary GT-1 motif (TTTTTC) elements are also indicated. B, The *DblycB2* gene possesses a GT-rich region in the first intron, which is potentially salt inducible (Li et al., 2010; Lu et al., 2011).

Different Induction Characteristics of *crts* Might Correlate with Regulatory Sequence Architecture

Previously, we isolated the promoter region of *Dbpsy* and found a cis-acting element candidate nominated as the GT-1 motif potentially involved in the hyperosmotic expression of *psy* (Lao et al., 2011). We believed that some vital CRTs responsible for β-carotene biosynthesis would be up-regulated under hyperosmolarity exerted by salt stress. Therefore, we isolated other *crts* promoters including *Dbzds*, *Dbpds*, and *DblycB1* (however, we failed to isolate the *DblycB2* promoter) in this study, with the expectation of mining cis-acting elements in response to salt stress similar to that of the *psy* promoter. To our surprise, an HSE cis-acting element in response to hypoosmolarity was found in the *Dbzds* promoter region. We repeated isolating the promoter and amplified a fragment overlapping the 5′ end of the *Dbzds* gene and the 3′ end of the *Dbzds* promoter region. The same sequence was obtained; thus, we believe that the obtained sequence is the upstream promoter region of *Dbzds*. Expression of BLE-EGFP under the control of this promoter further confirmed the promoter activity (Supplemental Fig. S2).

Different expression of *crts* (Fig. 5) implies differential and complex regulation mechanisms underlying the synergism in response to hyposalinity and hypersalinity among PSY, PDS, LYCB, and ZDS in the carotenogenesis pathway of *D. bardawil*. Obviously, *Dbpds* is not induced by salt stress; our previously isolated paralog *DblycB2* (Zhu et al., 2008) is not induced in most of the salt spectrum except for extreme hyperosmolarity (4.5 M), while *Dbzds*, *Dbpsy*, and *DblycB1* are greatly induced, as shown in Figure 5. We believe that different induction characteristics of these *crts* correlate with promoter architecture. Thus, we in silico analyzed and compared four promoters that we successfully isolated previously. The salt-inducible GT-1 motif is shared both by *Dbpsy* and *DblycB1* promoters but is absent from other *crts* promoters; otherwise, only *Dbzds* preserves the distinctive HRE in its promoter region (Fig. 7A). These findings implied that the salt inducibility of both *Dbpsy* and *DblycB1* and the hypoosmotic pattern of *Dbzds* potentially correlate with their unique cis-acting elements. Deletion experiments illuminated the authentic function of the HRE motif in the *Dbzds* promoter (Fig. 6). Loss of the hypoosmotic expression of *ble-egfp* driven by the HRE-deleted promoter (pDBET1) versus the *Dbzds* promoter (pZBET) was observed. Although GBF5BS is found downstream of HRE in the *Dbzds* promoter and also downstream of HRE in the *proDH* gene promoter (Satoh et al., 2002, 2004), deletion of GBF5BS (pDBET2) does not influence *ble-egfp* transcripts (Fig. 6). Hypoosmotic expression of *Dbzds* is exclusively attributed to HRE in the promoter region.

During the isolation and analysis of *crts* genomic structures, we found that the first intron of *DblycB2* contains a GT-rich region (Fig. 7B) first discovered and confirmed to be salt inducible in the *D. salina duplicated carbonic anhydrase1* (*Dsdca1*) promoter (Li et al., 2010; Lu et al., 2011). DsDCA is a plasma membrane salt-inducible protein characterized by its distinct ability to preserve activity over a broad range of salinities, while its counterparts from other species and other halophilic proteins require high salinity for conformation stability (Fisher et al., 1994, 1996; Premkumar et al., 2003). *DblycB2* is more similar to *Dsdca1*, and it might play an essential role in basal carotenoid biosynthesis vital for cell survival in a wide range of salinities, whereas *DblycB1* in combination with *DblycB2* (both are substantially induced in 4.5 M NaCl concentration; Fig. 5) might be required for a sufficient response of the cell to overcome reactive oxygen species caused by extreme hypersalinity (Chen et al., 2009). Although we failed to compare the cis-acting element differences between the two paralogs and we have not yet confirmed the potential GT-1 motif in the *DblycB1* promoter, evidence from our study implies at least that the regulation differences between *DblycB1* and *DblycB2* in response to different salinities might be attributed to potential salt-responsive elements, including cis-acting elements like the GT-1 motif and potential intron elements such as the GT-rich salt-inducible element, since intron enhancer and intronic regulatory elements can dramatically stimulate gene expression in *C. reinhardtii* (Lumbreras et al., 1998).

As discussed above, higher plants such as tomato, *Citrus* species, maize, and rice contain more than one *psy* or *lycB* paralog with differential regulation in different tissues in response to different environmental stimuli (Pecker et al., 1996; Fraser et al., 1999; Ronen et al., 2000; Ikoma et al., 2001; Li et al., 2008; Welsch et al., 2008). *Zmpsy3* mRNA increases with carotenoid accumulation under ABA stress, whereas *Zmpsy1* mRNA is not induced (Li et al., 2008). Rice *psy3* transcripts are upregulated during increasing ABA formation upon salt treatment and drought (Welsch et al., 2008). The *psy* gene duplication leads to subfunctionalization, with each paralog exhibiting differential gene expression (Li et al., 2008). The regulatory differences of paralogous *psy* genes derive from differences of cis-acting elements in the corresponding promoter regions, with light-responsive elements for *Ospsy1* and *Ospsy2* and an ABA response element as well as a coupling element for *Ospsy3* (Welsch et al., 2008). *D. salina* and *D. bardawil* both have two classes of *psy* as well, implying that carotenoid biosynthesis in these algae is differentially regulated in response to development and environmental stress (Tran et al., 2009). Furthermore, EST profiling in hypersaline shocked *D. salina* revealed a third EST of *pds* isogenes (Alkayal et al., 2010). Therefore, despite only one copy of *pds* and *zds* being reported currently, we cannot rule out the possibility of paralog(s) in *D. bardawil*, since genomic information is unavailable in *D. salina* and *D. bardawil* at present. Different induction characteristics of *crts* and their paralog(s), if they exist, might correlate with promoter and/or other regulatory sequence architecture, considering a potential salt-inducible GT-rich intron exclusively found in the *DblycB2* gene in comparison with *DlycB1* (Fig. 7B).

MATERIALS AND METHODS

Strains and Culture Conditions

Dunaliella bardawil strain 847 was obtained from the Institute of Hydrobiology, Chinese Academy of Science. Cells of *D. bardawil* were cultivated in defined medium (Zhu and Jiang, 2008; Chen et al., 2009) containing 2 M NaCl, 5 mM KNO_3, 0.1 mM $NaH_2PO_4 \cdot 2H_2O$, 5 mM $MgSO_4 \cdot 7H_2O$, 1 mM KCl, 10 mM $NaHCO_3$, and 0.3 mM $CaCl_2 \cdot 2H_2O$. The other materials used were 1 mL L^{-1} trace elements stock with 16.2 mM H_3BO_3, 9.1 mM $MnCl_2 \cdot 4H_2O$, 0.77 mM $ZnSO_4 \cdot 7H_2O$, 0.32 mM $CuSO_4 \cdot 5H_2O$, 0.1 mM Na_2MoO_4, and 9 mM $MnSO_4 \cdot 7H_2O$ as well as 0.5 mL L^{-1} iron-salting liquid stock with 0.56 mM $Na_2EDTA \cdot 2H_2O$ and 0.77 mM $FeCl_3 \cdot 6H_2O$. The pH of the medium after the addition of 100 mM Tris buffer was adjusted to 7.5 with 2 M HCl. *D. bardawil* cells were cultivated in a controlled chamber for 10 d (exponential phase) at 26°C and 8,000 lux provided by cool-white fluorescent lamps under a 16/8-h light/dark cycle with shaking at 96 rpm. These parameters were regarded as the normal condition (2 M NaCl). For semisolid culture, semisolid medium was made by adding 0.7 g L^{-1} Phytal gel (Sigma) to 25 mL of liquid medium; about 10^7 transformed cells were then plated and cultured for about 14 d under the normal condition without shaking. For stress treatment, 10^6 exponential phase cells cultivated in the normal condition were harvested by centrifugation at 5,000*g* for 8 min at 26°C, transferred to 100 mL of fresh medium containing 0, 1, 2, 3, and 4.5 M NaCl, and cultivated for 21 d (log or late log phase) under the normal condition as above for further experiments. Approximately 10^7 cells in log or late log phase were used for

real-time quantitative PCR experiments. For the expression study of *ble-egfp*, about 10^6 nuclear transformed cells exponentially cultured in 2 M salinity medium under the normal condition were harvested by centrifugation at 5,000*g* for 8 min at 26°C. Then the algal pellets were transferred to 100 mL of fresh medium in different salinities as above, and growth was resumed for 21 d for real-time quantitative PCR assay. *Escherichia coli* GT116 was used as the host for the multiplication of plasmids.

Cell Growth and Nitrate Content Analysis

D. bardawil cell growth in different salt stresses was measured daily according to our previous method (Zhu and Jiang, 2008; Chen et al., 2009). Briefly, the absorbance of each NaCl concentration of cultures was read at 630 nm in a spectrophotometer, and a corresponding concentration of blank medium without algal cells was used as the control sample. From the relationship curve between the optical density at 630 nm (OD_{630}) and the cell number regression equation, which was described in our previous work (Zhu and Jiang, 2008), the cell number was obtained by determining OD_{630}: $y = 899.08x - 12.544$, $r^2 = 0.9992$, where y = cell number ($\times 10^4$) and $x = OD_{630}$ value.

Nitrate concentration in the media with different salinities was detected according to Coesel et al. (2008). Specifically, cells recovered from 100 μL of culture were mixed thoroughly with 900 μL of 13% (w/v) NaCl and 20 μL of 1 M HCl. Nitrate was quantified photometrically using the equation $[NO_3^-]$ (mM) = $((A_{220} - A_{275}) - 0.0093) \times 3.558$.

Extraction of Genomic DNA and Total RNA

Genomic DNA extraction from cells in the log or late log phase was performed according to the method described by Mishra et al. (2008). Total RNA was extracted from approximately 10^7 *D. bardawil* cells grown at the log or late log phase using the E.Z.N.A. Total RNA Kit II (Omega) following the conditions recommended by the manufacturer.

Identification of *crts* Genomic DNA

We failed to directly clone the *crts* promoters using primer sets designed according to the 5′ untranslated regions of *crts* because of their relative short length for ideal genome-walking gene-specific primers. Therefore, genome walking was implemented first, with gene-specific primers to identify the genomic DNA of *crts* including *Dbzds*, *Dbpds*, and *DblycB1*. After the full-length *crts* genomic DNAs were obtained, promoter isolation was conducted using these genomic DNAs as templates. The cloning strategy is shown in Supplemental Figure S4. For *Dbpds*, the first genome walking using a gene-specific primer set complemented with the 3′ untranslated region of *Dbpds* mRNA was initiated with the Genome Walking Kit (TaKaRa). Then, conserved domains were selected by aligning PDS protein sequences to design seminested PCR primers, and the partial sequence obtained by these seminested PCR primers was overlapped with the first genome-walking product. Finally, the third genome walking was conducted according to the seminested PCR product to isolate the full-length *Dbpds* gene. In order to isolate the promoter and terminator, two sets of gene-specific primers were designed and genome walking was carried out independently. For other *crts*, at least two genome-walking reactions were carried out. All primers used in this study are listed in Supplemental Table S1.

Sequence Analysis

Sequence analysis was performed using BLAST software (http://blast.ncbi.nlm.nih.gov/Blast.cgi). Component analysis of *crts* was calculated using DNAStar software 7.1.0. Promoter prediction was operated by PlantPAN (http://plantpan.mbc.nctu.edu.tw/). The terminator scan program Poly (A) Signal Miner (http://dnafsminer.bic.nus.edu.sg/) and RibEx (http://132.248.32.45/cgi-bin/ribex.cgi) were used to analyze the putative terminator sequences of *crts*.

Construction of Plasmids

The putative promoter and terminator fragments obtained from genome walking were ligated into pCR2.1 vectors and assigned as pZ3.5 and pT1.5, respectively. Subsequent cloning into pCR2.1 vectors was conducted, resulting in pZ2.8 and pT1.3 plasmids, with primers rendering *Asc*I and *Sac*II as well as *Sac*II and *Xho*I restriction sites to the ends of the supposed promoter and terminator in 5′ to 3′ orientation. The *egfp* coding sequence was amplified using pcDNA6 myc-his-EGFP B vector (kindly provided by Y.C. Cao, School of Biological Science and Engineering, South China University of Technology) as template. The *ble* coding sequence without the stop codon TAA was artificially synthesized using primers designed by DNAWorks (http://helixweb.nih.gov/dnaworks/). The *ble* coding sequence synthesis condition was as described by Dong et al. (2007a). The chimeric fragment of *ble-egfp* with *Asc*I and *Sac*II restriction sites in the corresponding ends was obtained by means of a two-step overlap PCR method (Heckman and Pease, 2007). The synthetic chimeric gene was then cloned into pZ2.8 plasmid cut by the same enzymes using conventional cloning techniques, producing the intermediate vector pZBE. Finally, expression vector pZBET was constructed by ligation of the hypothetic terminator fragment into the end of the chimeric gene of pZBE through conventional approaches. HRE-deleted vector pDBET1, GBF5BS-deleted vector pDBET2, and HRE- and GBF5BS-deleted vector pDBET3 were constructed by splice overlap extension-PCR using deletion primer sets (Supplemental Table S1). In brief, the negative control vector pET was also established by the TA cloning strategy. This strategy uses (1) non-template-dependent *Thermus aquaticus* polymerase to generate single 3′-A overhang PCR products by preferentially adding a single adenosine to the 3′ ends of a double-stranded DNA molecule; and (2) a linearized T-vector, which has single 3′-T overhangs on both ends, to allow direct, high-efficiency cloning of PCR products. Constructs used in this study are shown in Figure 4.

Nuclear Transformation of *D. bardawil*

A modified transformation method was used for the nuclear transformation of *D. bardawil* cells according to Sun et al. (2005). Briefly, cells were harvested in log or late log phase of growth (4–6 × 10^6 cells mL^{-1}) by centrifuging at 1,000*g* for 5 min, washed, and suspended twice to a final density of about 2 × 10^8 cells mL^{-1} in buffer B (1.4 M glycerol, 50 mM NaCl, 30 mM Tris-Cl, pH 7.5, and 6 mM $CaCl_2$). Recombinant plasmids (final concentration of 10 mg L^{-1}) and carrier DNA (final concentration of 200 mg L^{-1} sheared and denatured salmon sperm DNA) were added to 0.5 mL of the cell suspension and mixed; 100 μL of the mixture was moved to a prechilled disposable chamber (with a 2-mm gap) and kept on ice for 10 min before electroporation. Electroporation was performed using the Gene Pulser Xcell Electroporation System (Life Science) with an exponential electric pulse with electrical field strength of 1,000 V cm^{-1} at a capacitance of 1,000 μF. After transformation, the cells were kept on ice for 10 min and then added to 10 mL of liquid culture medium without antibiotics for a 12-h incubation at 25°C in the dark. After the incubation, cells were cultured in the normal condition discussed above.

Selection of Positive Transformants and Nonselective Culture

To select Zeocin (Invitrogen) resistance in cells of transgenic *D. bardawil*, about 10^7 transformed cells were immediately plated on semisolid culture medium containing 10 mg L^{-1} Zeocin and cultured for about 14 d until small green colonies of the alga appeared. Five colonies of each transformant were picked out and inoculated into liquid culture containing 10 mg L^{-1} Zeocin and 2 M NaCl under the normal condition without shaking. When the transformed cells of *D. bardawil* grew to the log phase, the cells were collected and PCR and RT-PCR were implemented using the RNA PCR Kit (AMV) version 3.0 (TaKaRa) to screen the positive transformants using primers vBE For and vBE Rev. PCR parameters were as follows: 95°C for 5 min and then 35 cycles of 94°C for 45s, 60°C for 45s, and 72°C for 1 min. The PCR products were further confirmed by DNA sequencing. Positive transformants were grown in liquid medium devoid of Zeocin containing the different NaCl concentrations mentioned above for quantitative analysis.

Expression Studies of *crts* and *ble-egfp*

Real-time quantitative PCR was performed with a 7500 Real-Time PCR System (Applied Biosystems) using the PrimeScript RT Reagent Kit with gDNA Eraser (which supplies RNase-free DNase I to remove any coisolated genomic DNA) and the SYBR Green PCR Kit (product codes DRR041A and DRR047A, respectively; TaKaRa). Primers for quantitative analysis are listed in Supplemental Table S1. The reaction mix contained 4 μL of complementary DNA, 0.5 μL of forward and reverse primer mix (20 μM each), 1 μL of 50×

ROX Reference Dye II, and 25 μL of 2× TaKaRa SYBR Green PCR mix in a final volume of 50 μL. All reactions were set up in triplicate, and every sample was replicated in parallel three times to ensure statistical relevance. The following standard thermal conditions were used for all PCRs: 30 s at 95°C and then 40 cycles of 30 s at 95°C and 34 s at 60°C. Primer specificity was confirmed by RT-PCR amplification before real-time quantitative PCR, which produced single amplicons of the expected size for each primer set; these amplicons were sequenced to finally validate their specific amplification. The specificity of real-time quantitative PCR was monitored by the presence of dissociation curves with single peaks and sequencing of its products with unique bands of the expected sizes. Amplicon dissociation curves were obtained after cycle 40 with default settings suggested by the instrument. Data were analyzed using SDS software (Applied Biosystems). All quantifications were normalized to the amount of *D. bardawil glyceraldehyde-3-phosphate dehydrogenase* gene, the relative abundance of which was determined under salt stress, as an internal control.

Statistical Analysis

The data were processed by one-way ANOVA using SPSS version 13.0 (SPSS). Summary statistics were expressed as means ± SD. In all statistical analyses, $P < 0.05$ was considered statistically significant.

Supplemental Data

The following materials are available in the online version of this article.

Supplemental Figure S1. The genomic organization of *Dbzds*.

Supplemental Figure S2. Fluorescence images of *D. bardwil* transformants.

Supplemental Figure S3. Positive transformants screening and characterization.

Supplemental Figure S4. Cloning strategies for isolating *crts* genomic DNA.

Supplemental Table S1. Primers used in this study.

Received January 7, 2014; accepted February 20, 2014; published March 14, 2014.

LITERATURE CITED

Abreu-Goodger C, Merino E (2005) RibEx: a web server for locating riboswitches and other conserved bacterial regulatory elements. Nucleic Acids Res **33:** W690–W692

Al-Babili S, Hartung W, Kleinig H, Beyer P (1999) CPTA modulates levels of carotenogenic proteins and their mRNAs and affects carotenoid and ABA content as well as chromoplast structure in *Narcissus pseudonarcissus* flowers. Plant Biol **1:** 607–612

Albrecht M, Klein A, Hugueney P, Sandmann G, Kuntz M (1995) Molecular cloning and functional expression in *E. coli* of a novel plant enzyme mediating ζ-carotene desaturation. FEBS Lett **372:** 199–202

Alkayal F, Albion RL, Tillett RL, Hathwaik LT, Lemos MS, Cushman JC (2010) Expressed sequence tag (EST) profiling in hyper saline shocked *Dunaliella salina* reveals high expression of protein synthetic apparatus components. Plant Sci **179:** 437–449

Amotz AB, Katz A, Avron M (1982) Accumulation of β-carotene in halotolerant algae: purification and characterization of β-carotene-rich globules from *Dunaliella bardawil*. J Phycol **18:** 529–537

Babu MA, Singh D, Gothandam K (2011) Effect of salt stress on expression of carotenoid pathway genes in tomato. J Stress Physiol Biochem **7:** 87–94

Bartley GE, Scolnik PA, Beyer P (1999) Two *Arabidopsis thaliana* carotene desaturases, phytoene desaturase and ζ-carotene desaturase, expressed in *Escherichia coli*, catalyze a poly-cis pathway to yield pro-lycopene. Eur J Biochem **259:** 396–403

Bautista JA, Rappaport F, Guergova-Kuras M, Cohen RO, Golbeck JH, Wang JY, Béal D, Diner BA (2005) Biochemical and biophysical characterization of photosystem I from phytoene desaturase and ζ-carotene desaturase deletion mutants of Synechocystis sp. PCC 6803: evidence for PsaA- and PsaB-side electron transport in cyanobacteria. J Biol Chem **280:** 20030–20041

Borghesi E, González-Miret ML, Escudero-Gilete ML, Malorgio F, Heredia FJ, Meléndez-Martínez AJ (2011) Effects of salinity stress on carotenoids, anthocyanins, and color of diverse tomato genotypes. J Agric Food Chem **59:** 11676–11682

Borowitzka MA, Borowitzka LJ, Kessly D (1990) Effects of salinity increase on carotenoid accumulation in the green alga *Dunaliella salina*. J Appl Phycol **2:** 111–119

Breitenbach J, Fernández-González B, Vioque A, Sandmann G (1998) A higher-plant type ζ-carotene desaturase in the cyanobacterium *Synechocystis* PCC6803. Plant Mol Biol **36:** 725–732

Chen H, Jiang JG (2009) Osmotic responses of *Dunaliella* to the changes of salinity. J Cell Physiol **219:** 251–258

Chen H, Jiang JG, Wu GH (2009) Effects of salinity changes on the growth of *Dunaliella salina* and its isozyme activities of glycerol-3-phosphate dehydrogenase. J Agric Food Chem **57:** 6178–6182

Cheong YH, Moon BC, Kim JK, Kim CY, Kim MC, Kim IH, Park CY, Kim JC, Park BO, Koo SC, et al (2003) BWMK1, a rice mitogen-activated protein kinase, locates in the nucleus and mediates pathogenesis-related gene expression by activation of a transcription factor. Plant Physiol **132:** 1961–1972

Chinnusamy V, Ohta M, Kanrar S, Lee BH, Hong X, Agarwal M, Zhu JK (2003) ICE1: a regulator of cold-induced transcriptome and freezing tolerance in *Arabidopsis*. Genes Dev **17:** 1043–1054

Coesel SN, Baumgartner AC, Teles LM, Ramos AA, Henriques NM, Cancela L, Varela JCS (2008) Nutrient limitation is the main regulatory factor for carotenoid accumulation and for *Psy* and *Pds* steady state transcript levels in *Dunaliella salina* (Chlorophyta) exposed to high light and salt stress. Mar Biotechnol (NY) **10:** 602–611

Després C, Chubak C, Rochon A, Clark R, Bethune T, Desveaux D, Fobert PR (2003) The *Arabidopsis* NPR1 disease resistance protein is a novel cofactor that confers redox regulation of DNA binding activity to the basic domain/leucine zipper transcription factor TGA1. Plant Cell **15:** 2181–2191

Ding J, Li X, Hu H (2012) Systematic prediction of cis-regulatory elements in the *Chlamydomonas reinhardtii* genome using comparative genomics. Plant Physiol **160:** 613–623

Dong B, Mao R, Li B, Liu Q, Xu P, Li G (2007a) An improved method of gene synthesis based on DNAWorks software and overlap extension PCR. Mol Biotechnol **37:** 195–200

Dong H, Deng Y, Mu J, Lu Q, Wang Y, Xu Y, Chu C, Chong K, Lu C, Zuo J (2007b) The *Arabidopsis* Spontaneous Cell Death1 gene, encoding a ζ-carotene desaturase essential for carotenoid biosynthesis, is involved in chloroplast development, photoprotection and retrograde signalling. Cell Res **17:** 458–470

Drocourt D, Calmels T, Reynes JP, Baron M, Tiraby G (1990) Cassettes of the *Streptoalloteichus hindustanus* ble gene for transformation of lower and higher eukaryotes to phleomycin resistance. Nucleic Acids Res **18:** 4009

Duan HK, Zhu Y, Qi DD, Li WL, Hua XJ, Liu YX, Deng X (2012) Comparative study on the expression of genes involved in carotenoid and ABA biosynthetic pathway in response to salt stress in tomato. J Integr Agric **11:** 1093–1102

Fambrini M, Salvini M, Conti A, Michelotti V, Pugliesi C (2004) Expression of the ζ-carotene desaturase gene in sunflower. Plant Biosyst **138:** 203–206

Farré G, Sanahuja G, Naqvi S, Bai C, Capell T, Zhu C, Christou P (2010) Travel advice on the road to carotenoids in plants. Plant Sci **179:** 28–48

Feltl L, Pacakova V, Stulik K, Volka K (2005) Reliability of carotenoid analyses: a review. Curr Anal Chem **1:** 93–102

Fisher M, Gokhman I, Pick U, Zamir A (1996) A salt-resistant plasma membrane carbonic anhydrase is induced by salt in *Dunaliella salina*. J Biol Chem **271:** 17718–17723

Fisher M, Pick U, Zamir A (1994) A salt-induced 60-kilodalton plasma membrane protein plays a potential role in the extreme halotolerance of the alga *Dunaliella*. Plant Physiol **106:** 1359–1365

Fraser PD, Enfissi EM, Halket JM, Truesdale MR, Yu D, Gerrish C, Bramley PM (2007) Manipulation of phytoene levels in tomato fruit: effects on isoprenoids, plastids, and intermediary metabolism. Plant Cell **19:** 3194–3211

Fraser PD, Kiano JW, Truesdale MR, Schuch W, Bramley PM (1999) Phytoene synthase-2 enzyme activity in tomato does not contribute to carotenoid synthesis in ripening fruit. Plant Mol Biol **40:** 687–698

Fujimoto SY, Ohta M, Usui A, Shinshi H, Ohme-Takagi M (2000) *Arabidopsis* ethylene-responsive element binding factors act as transcriptional

activators or repressors of GCC box-mediated gene expression. Plant Cell **12:** 393–404

Girin T, Lejay L, Wirth J, Widiez T, Palenchar PM, Nazoa P, Touraine B, Gojon A, Lepetit M (2007) Identification of a 150 bp cis-acting element of the *AtNRT2.1* promoter involved in the regulation of gene expression by the N and C status of the plant. Plant Cell Environ **30:** 1366–1380

Goodwin TW (1980) The Biochemistry of the Carotenoids, Vol I. Chapman and Hall, New York

Grünewald K, Eckert M, Hirschberg J, Hagen C (2000) Phytoene desaturase is localized exclusively in the chloroplast and up-regulated at the mRNA level during accumulation of secondary carotenoids in *Haematococcus pluvialis* (Volvocales, Chlorophyceae). Plant Physiol **122:** 1261–1268

Hart CM, Nagy F, Meins F Jr (1993) A 61 bp enhancer element of the tobacco β-1,3-glucanase B gene interacts with one or more regulated nuclear proteins. Plant Mol Biol **21:** 121–131

Heckman KL, Pease LR (2007) Gene splicing and mutagenesis by PCR-driven overlap extension. Nat Protoc **2:** 924–932

Hirschberg J (2001) Carotenoid biosynthesis in flowering plants. Curr Opin Plant Biol **4:** 210–218

Ikoma Y, Komatsu A, Kita M, Ogawa K, Omura M, Yano M, Moriguchi T (2001) Expression of a phytoene synthase gene and characteristic carotenoid accumulation during citrus fruit development. Physiol Plant **111:** 232–238

Johnson EA, Schroeder WA, Fiechter A (1995) Advances in biochemical engineering, biotechnology. *In* EA Johnson, WA Schroeder, eds, Microbial Carotenoids, Vol 53. Springer, Berlin, pp 119–178

Kim SH, Kim YH, Ahn YO, Ahn MJ, Jeong JC, Lee HS, Kwak SS (2013) Downregulation of the lycopene ε-cyclase gene increases carotenoid synthesis via the β-branch-specific pathway and enhances salt-stress tolerance in sweetpotato transgenic calli. Physiol Plant **147:** 432–442

Lam E, Benfey PN, Gilmartin PM, Fang RX, Chua NH (1989) Site-specific mutations alter in vitro factor binding and change promoter expression pattern in transgenic plants. Proc Natl Acad Sci USA **86:** 7890–7894

Landrum JT, Bone RA (2001) Lutein, zeaxanthin, and the macular pigment. Arch Biochem Biophys **385:** 28–40

Lao YM, Xiao L, Ye ZW, Jiang JG, Zhou SS (2011) *In silico* analysis of phytoene synthase and its promoter reveals hints for regulation mechanisms of carotenogenesis in *Dunaliella bardawil*. Bioinformatics **27:** 2201–2208

Lers A, Biener Y, Zamir A (1990) Photoinduction of massive β-carotene accumulation by the alga *Dunaliella bardawil*: kinetics and dependence on gene activation. Plant Physiol **93:** 389–395

Li F, Vallabhaneni R, Wurtzel ET (2008) PSY3, a new member of the phytoene synthase gene family conserved in the Poaceae and regulator of abiotic stress-induced root carotenogenesis. Plant Physiol **146:** 1333–1345

Li J, Lu Y, Xue L, Xie H (2010) A structurally novel salt-regulated promoter of duplicated carbonic anhydrase gene 1 from *Dunaliella salina*. Mol Biol Rep **37:** 1143–1154

Li M, Gan Z, Cui Y, Shi C, Shi X (2011) Cloning and characterization of the ζ-carotene desaturase gene from *Chlorella protothecoides* CS-41. J Biomed Biotechnol **2011:** 731542

Li Y, Huang J, Sandmann G, Chen F (2009) High-light and sodium chloride stress differentially regulate the biosynthesis of astaxanthin in *Chlorella zofingiensis* (Chlorophyceae). J Phycol **45:** 635–641

Linden H, Misawa N, Saito T, Sandmann G (1994) A novel carotenoid biosynthesis gene coding for ζ-carotene desaturase: functional expression, sequence and phylogenetic origin. Plant Mol Biol **24:** 369–379

Linden H, Vioque A, Sandmann G (1993) Isolation of a carotenoid biosynthesis gene coding for ζ-carotene desaturase from *Anabaena* PCC 7120 by heterologous complementation. FEMS Microbiol Lett **106:** 99–103

Lu Y, Li J, Xue L, Yan H, Yuan H, Wang C (2011) A duplicated carbonic anhydrase 1 (DCA1) promoter mediates the nitrate reductase gene switch of *Dunaliella salina*. J Appl Phycol **23:** 673–680

Lumbreras V, Stevens DR, Purton S (1998) Efficient foreign gene expression in *Chlamydomonas reinhardtii* mediated by an endogenous intron. Plant J **14:** 441–447

Maass D, Arango J, Wüst F, Beyer P, Welsch R (2009) Carotenoid crystal formation in *Arabidopsis* and carrot roots caused by increased phytoene synthase protein levels. PLoS ONE **4:** e6373–e6384

Matthews PD, Luo RB, Wurtzel ET (2003) Maize phytoene desaturase and ζ-carotene desaturase catalyse a poly-Z desaturation pathway: implications for genetic engineering of carotenoid content among cereal crops. J Exp Bot **54:** 2215–2230

Michaud DS, Feskanich D, Rimm EB, Colditz GA, Speizer FE, Willett WC, Giovannucci E (2000) Intake of specific carotenoids and risk of lung cancer in 2 prospective US cohorts. Am J Clin Nutr **72:** 990–997

Mishra A, Mandoli A, Jha B (2008) Physiological characterization and stress-induced metabolic responses of *Dunaliella salina* isolated from salt pan. J Ind Microbiol Biotechnol **35:** 1093–1101

Mohanty B, Krishnan SPT, Swarup S, Bajic VB (2005) Detection and preliminary analysis of motifs in promoters of anaerobically induced genes of different plant species. Ann Bot (Lond) **96:** 669–681

Norris SR, Meyer SE, Callis J (1993) The intron of *Arabidopsis thaliana* polyubiquitin genes is conserved in location and is a quantitative determinant of chimeric gene expression. Plant Mol Biol **21:** 895–906

Pecker I, Gabbay R, Cunningham FX Jr, Hirschberg J (1996) Cloning and characterization of the cDNA for lycopene β-cyclase from tomato reveals decrease in its expression during fruit ripening. Plant Mol Biol **30:** 807–819

Premkumar L, Bageshwar UK, Gokhman I, Zamir A, Sussman JL (2003) An unusual halotolerant alpha-type carbonic anhydrase from the alga *Dunaliella salina* functionally expressed in *Escherichia coli*. Protein Expr Purif **28:** 151–157

Rabbani S, Beyer P, Lintig J, Hugueney P, Kleinig H (1998) Induced β-carotene synthesis driven by triacylglycerol deposition in the unicellular alga *Dunaliella bardawil*. Plant Physiol **116:** 1239–1248

Raja R, Hemaiswarya S, Rengasamy R (2007) Exploitation of *Dunaliella* for β-carotene production. Appl Microbiol Biotechnol **74:** 517–523

Ronen G, Carmel-Goren L, Zamir D, Hirschberg J (2000) An alternative pathway to β-carotene formation in plant chromoplasts discovered by map-based cloning of β and old-gold color mutations in tomato. Proc Natl Acad Sci USA **97:** 11102–11107

Sadka A, Lers A, Zamir A, Avron M (1989) A critical examination of the role of *de novo* protein synthesis in the osmotic adaptation of the halotolerant alga *Dunaliella*. FEBS Lett **244:** 93–98

Salguero A, León R, Mariotti A, de la Morena B, Vega JM, Vílchez C (2005) UV-A mediated induction of carotenoid accumulation in Dunaliella bardawil with retention of cell viability. Appl Microbiol Biotechnol **66:** 506–511

Sandmann G (2009) Evolution of carotene desaturation: the complication of a simple pathway. Arch Biochem Biophys **483:** 169–174

Satoh R, Fujita Y, Nakashima K, Shinozaki K, Yamaguchi-Shinozaki K (2004) A novel subgroup of bZIP proteins functions as transcriptional activators in hypoosmolarity-responsive expression of the *ProDH* gene in *Arabidopsis*. Plant Cell Physiol **45:** 309–317

Satoh R, Nakashima K, Seki M, Shinozaki K, Yamaguchi-Shinozaki K (2002) ACTCAT, a novel *cis*-acting element for proline- and hypoosmolarity-responsive expression of the *ProDH* gene encoding proline dehydrogenase in Arabidopsis. Plant Physiol **130:** 709–719

Schmidt-Dannert C (2000) Engineering novel carotenoids in microorganisms. Curr Opin Biotechnol **11:** 255–261

Shaish A, Harari A, Hananshvili L, Cohen H, Bitzur R, Luvish T, Ulman E, Golan M, Ben-Amotz A, Gavish D, et al (2006) 9-Cis β-carotene-rich powder of the alga *Dunaliella bardawil* increases plasma HDL-cholesterol in fibrate-treated patients. Atherosclerosis **189:** 215–221

Simkin AJ, Breitenbach J, Kuntz M, Sandmann G (2000) In vitro and in situ inhibition of carotenoid biosynthesis in *Capsicum annuum* by bleaching herbicides. J Agric Food Chem **48:** 4676–4680

Simkin AJ, Labouré AM, Kuntz M, Sandmann G (2003) Comparison of carotenoid content, gene expression and enzyme levels in tomato (*Lycopersicon esculentum*) leaves. Z Naturforsch C **58:** 371–380

Simpson SD, Nakashima K, Narusaka Y, Seki M, Shinozaki K, Yamaguchi-Shinozaki K (2003) Two different novel *cis*-acting elements of *erd1*, a *clpA* homologous Arabidopsis gene function in induction by dehydration stress and dark-induced senescence. Plant J **33:** 259–270

Steinbrenner J, Linden H (2001) Regulation of two carotenoid biosynthesis genes coding for phytoene synthase and carotenoid hydroxylase during stress-induced astaxanthin formation in the green alga *Haematococcus pluvialis*. Plant Physiol **125:** 810–817

Sun G, Sui Z, Zhang X (2008) Cloning and characterization of the phytoene desaturase (*pds*) gene: a key enzyme for carotenoids synthesis in *Dunaliella* (Chlorophyta). J Ocean Univ China **7:** 311–318

Sun Y, Yang Z, Gao X, Li Q, Zhang Q, Xu Z (2005) Expression of foreign genes in *Dunaliella* by electroporation. Mol Biotechnol **30:** 185–192

Tran D, Haven J, Qiu WG, Polle JEW (2009) An update on carotenoid biosynthesis in algae: phylogenetic evidence for the existence of two classes of phytoene synthase. Planta **229:** 723–729

Tuan PA, Kim JK, Lee S, Chae SC, Park SU (2013) Molecular characterization of carotenoid cleavage dioxygenases and the effect of gibberellin, abscisic acid, and sodium chloride on the expression of genes involved in the carotenoid biosynthetic pathway and carotenoid accumulation in the callus of *Scutellaria baicalensis* Georgi. J Agric Food Chem **61:** 5565–5572

Veeranagamallaiah G, Jyothsnakumari G, Thippeswamy M, Chandra Obul Reddy P, Surabhi GK, Sriranganayakulu G, Mahesh Y, Rajasekhar B, Madhurarekha C, et al (2008) Proteomic analysis of salt stress responses in foxtail millet (*Setaria italica* L. cv. Prasad) seedlings. Plant Sci **175:** 631–641

Walter MH, Strack D (2011) Carotenoids and their cleavage products: biosynthesis and functions. Nat Prod Rep **28:** 663–692

Wang R, Guan P, Chen M, Xing X, Zhang Y, Crawford NM (2010) Multiple regulatory elements in the Arabidopsis NIA1 promoter act synergistically to form a nitrate enhancer. Plant Physiol **154:** 423–432

Welsch R, Wüst F, Bär C, Al-Babili S, Beyer P (2008) A third phytoene synthase is devoted to abiotic stress-induced abscisic acid formation in rice and defines functional diversification of phytoene synthase genes. Plant Physiol **147:** 367–380

Ye ZW, Jiang JG (2010) Analysis of an essential carotenogenic enzyme: ζ-carotene desaturase from unicellular alga *Dunaliella salina*. J Agric Food Chem **58:** 11477–11482

Ye ZW, Liu GN, Jiang JG (2011) Structural and phylogenetic analysis of a novel ζ-carotene desaturase from *Dunaliella bardawil*, a unicellular alga that accumulates large amounts of β-carotene. Limnol Oceanogr **56:** 133–138

Zhu YH, Jiang JG (2008) Continuous cultivation of *Dunaliella salina* in photobioreactor for the production of β-carotene. Eur Food Res Technol **227:** 953–959

Zhu YH, Jiang JG, Chen Q (2008) Characterization of cDNA of lycopene β-cyclase responsible for a high level of β-carotene accumulation in *Dunaliella salina*. Biochem Cell Biol **86:** 285–292

Zhu YH, Jiang JG, Chen XW (2007) cDNA for phytoene desaturase in *Dunaliella salina* and its expressed protein as indicators of phylogenetic position of the β-carotene biosynthetic pathway. J Sci Food Agric **87:** 1772–1777